Supramolecular Chemistry
Publication details, including instructions for authors and subscription information:
http://www.informaworld.com/smpp/title~content=t713649759

Tren-spaced rhodamine and pyrene fluorophores: Excimer modulation with metal ion complexation

Min Hee Lee[a]; Guipeun Kang[b]; Jong Wan Kim[c]; Sihyun Ham[b]; Jong Seung Kim[a]
[a] Department of Chemistry, Korea University, Seoul, South Korea [b] Department of Chemistry, Sookmyung Women's University, Seoul, South Korea [c] Department of Laboratory Medicine, Dankook University College of Medicine, Cheonan, South Korea

To cite this Article Lee, Min Hee , Kang, Guipeun , Kim, Jong Wan , Ham, Sihyun and Kim, Jong Seung(2009) 'Tren-spaced rhodamine and pyrene fluorophores: Excimer modulation with metal ion complexation', Supramolecular Chemistry, 21: 1, 135 — 141
To link to this Article: DOI: 10.1080/10610270802527069
URL: http://dx.doi.org/10.1080/10610270802527069

Supramolecular Chemistry
Vol. 21, Nos. 1–2, January–March 2009, 135–141

Taylor & Francis
Taylor & Francis Group

Tren-spaced rhodamine and pyrene fluorophores: Excimer modulation with metal ion complexation

Min Hee Lee[a], Guipeun Kang[b], Jong Wan Kim[c], Sihyun Ham[b]* and Jong Seung Kim[a]*

[a]*Department of Chemistry, Korea University, Seoul, South Korea;* [b]*Department of Chemistry, Sookmyung Women's University, Seoul, South Korea;* [c]*Department of Laboratory Medicine, Dankook University College of Medicine, Cheonan, South Korea*

(*Received 28 July 2008; final version received 11 September 2008*)

A new chromogenic and fluorogenic probe (**1**) exhibits a significant selectivity towards Cu(II) and Hg(II) ions to give the modulation of pyrene (Py) excimer emission. Also, its sensing behaviours towards Cu(II) and Hg(II) ions were investigated experimentally and computationally. Hg(II) complexation induces the ring opening of the rhodamine spirolactam unit of **1** and shows enhanced dynamic excimer emission. Cu(II), on the other hand, is found to be encapsulated in the Py amide group to provide a static excimer emission. Hg(II) in the Hg(II)·**1** complex can be readily replaced by Cu(II), and then the static excimer emission of two Pys in **1** is reformed.

Keywords: pyrene; rhodamine; static excimer; copper; mercury

Introduction

The design and synthesis of fluorescent sensors have become increasingly important in the environmental systems (*1*). To date, considerable attention of many heavy and transition metal ions, e.g. Cu(II), Hg(II), Zn(II) and Pb(II), has been received in the frame of the development of the new molecular sensors because of their essential and deleterious roles. An effective fluorescent sensor must convert selective cation recognition into an easily monitored and highly sensitive light signal from the fluorophore (*2*, *3*). In most cases, however, a Cu(II) ion sensor is known to encounter an interference of Hg(II) ion (*4*). Then, it has been suggested to synthesise a receptor that can discriminate the Cu(II) over Hg(II) ion in competition experiments with respect to fluorescence changes.

As a fluorogenic unit, pyrene (Py) has been attractive mainly due to its characteristic excimer formation (*5*, *6*). There is not only the possibility of conventional *dynamic* excimer formation resulting from the sandwich-type interaction of the Py dimer in the excited state, but also that of *static* excimer formation produced by the partial overlap of Py moeties (*7*).

Rhodamine dyes are another class of efficient fluorophores having two isomers. The spirocyclic-form isomer of the rhodamine is generally non-fluorescent and colourless. However, the ring opening of the spirolactam induces highly conjugated quinonoid rhodamine, which is pink and strongly fluorescent (*8*).

With such physical properties of Py and rhodamine in mind, we have prepared a molecule in which two Pys and the rhodamine are anchored by a multidentate ligand, tren (tris(2-aminoethyl)amine). Here, we report on the selective sensing properties of **1** for Cu(II) even in the presence of Hg(II) with respect to fluorescence changes of both the rhodamine and Py excimers. Additionally, the results of the density function theory (DFT) calculation are also presented to support the binding mechanism and fluorescence changes of **1** upon Cu(II) complexation.

Results and discussion

As shown in Scheme 1, **1** was prepared by a coupling reaction of 1-pyrenebutyric acid with **3** using N,N′-dicyclohexyl carbodiimide (DCC) and a catalytic amount of 4-dimethylaminopyridine (DMAP) in THF. For the comparison of photochemical properties of **1**, reference **2** was also prepared via a similar synthetic route to **1**.

In Figure 1(a), the CH_3CN solution of **1** displays intensive absorption bands at 273, 324 and 340 nm intrinsically originated from the Py units. The addition of Cu(II) to the solution of **1** produces red shifts in the maxima to 275 ($\Delta\lambda = 2$ nm), 337 ($\Delta\lambda = 13$ nm) and 350 nm ($\Delta\lambda = 10$ nm), because there is a marked $\pi-\pi$ stacking interaction between the two Pys (*7*). On the other hand, a solution of **1** changes the colour to pink and shows a new band at 555 nm by the addition of Hg(II) or Pb(II), which is induced by the ring opening (*9*) of the rhodamine upon metal ion binding.

With an excitation at 340 nm, **1** exhibits both pyrenyl monomer and excimer emissions at 376 and 475 nm, respectively (Figure 1(b)). The addition of Cu(II) ion

*Corresponding authors. Email: sihyun@sookmyung.ac.kr; jongskim@korea.ac.kr

ISSN 1061-0278 print/ISSN 1029-0478 online

DOI: 10.1080/10610270802527069
http://www.informaworld.com

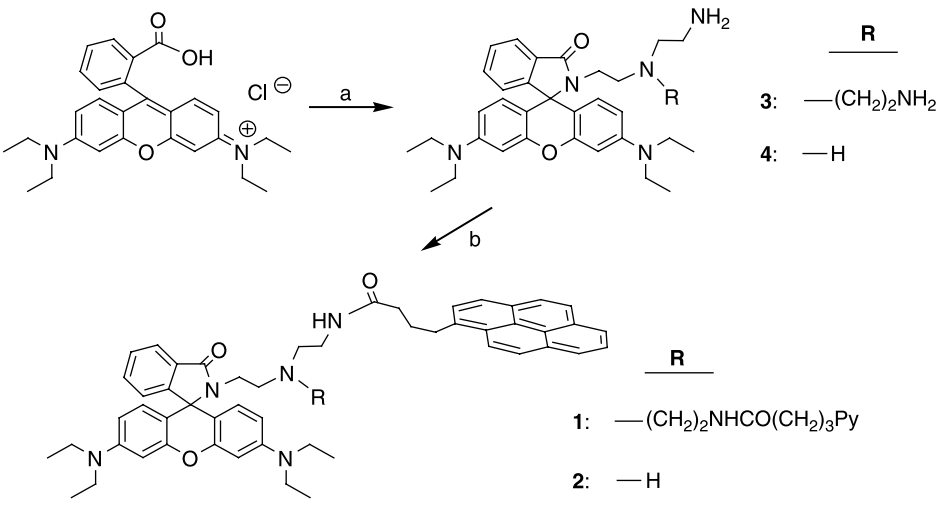

Scheme 1. Synthetic pathways of **1**–**4**. Conditions: (a) MeOH, tris(2-aminoethyl)amine or diethylenetriamine, reflux; (b) 1-pyrenebutyric acid, DCC, DMAP, THF, rt.

induces an increase in both the monomer and excimer intensities of **1**. Besides, the corresponding wavelengths of the monomer and excimer emissions are red-shifted to 382 nm ($\Delta\lambda = 6$ nm) and blue-shifted to 441 nm ($\Delta\lambda = 34$ nm), respectively. However, in the presence of Hg(II) or Pb(II) ion, a *dynamic* excimer of the Py increases, whereas no wavelength shift is observed. Compound **1** was also excited at 520 nm, corresponding to the UV/vis absorption of the rhodamine (Figure S1, available online).

In general, for the complexation of Cu(II) or Hg(II) ion, Py fluorescence is quenched due to the heavy metal effect (*4*, *7b*). However, we found that, in this system, pyrenyl fluorescence of **1** is not quenched by the addition of excess Cu(II) or Hg(II) ion, but its excimer emission band is shifted by Cu(II) addition due to static excimer formation and is enhanced by Hg(II).

Table 1 summarises the absorption and fluorescence features (λ_{abs}, ε, and λ^{a}_{em}) of **1** and also lists the association constants (K^{c}_{a}) [2] and quantum yields (Φ^{d}_{f})[1] (*10*) of **1** for the Cu(II) and Hg(II) ions, respectively.

The absorption bands of **1** are red-shifted upon addition of Cu(II) ion (Figure 2(a)). In the other aspect of the selective sensing Cu(II) ion, we noted in our experiment that the colour change of **1** is dependent on the metal:ligand mole ratio. With the addition of one equivalent of Cu(II) ion, the colourless solution of **1** becomes pink, which is due to the metal ion-induced ring opening of the rhodamine. Upon further addition of Cu(II) ion to a solution of **1**, the absorption band at 554 nm disappears and also the colour changes from pink to pale brown (Figure S2). For these unexpected events, we assume that in **1**, there are two different kinds of binding sites: carboxyl oxygen of tren and carboxyl oxygen of the rhodamine. The first one of Cu(II) ion is bound to the rhodamine part, and then the next one is in turn encapsulated in the tren part (*11*), which can be more rationalised by the DFT calculation (*vide infra*). This assumption is also in good agreement with the mass spectrum data (1:1 stoichiometry), which is obtained by the addition of excess $Cu(ClO_4)_2$ (Figures S3–S5, available online).

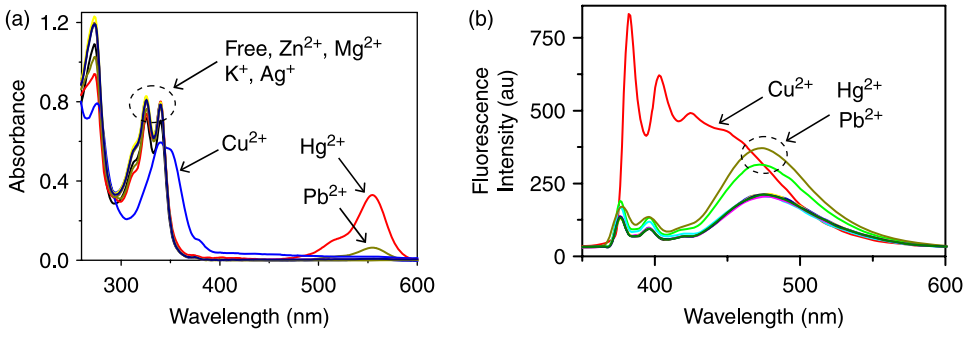

Figure 1. (a) Absorption (20.0 μM) and (b) fluorescence (6.0 μM) spectra of **1** upon addition of ClO_4^- salts of Hg^{2+}, Pb^{2+}, Zn^{2+}, Cu^{2+}, Mg^{2+}, K^+ and Ag^+(100 equiv., respectively) in CH_3CN, $\lambda_{ex} = 340$ nm.

Table 1. Photophysical properties of **1**: association constants (K_a[a]), maximum absorption wavelength (λ_{abs}), maximum emission wavelength (λ_{em}), extinction coefficients (ε) and quantum yields (Φ_f[b]) of **1** for Cu(II) and Hg(II).

Entry	λ_{abs} (nm)	ε (M^{-1} cm^{-1})	λ_{em} (nm)[c]	K_a (M^{-1})[a]	λ_{ex} (nm)[b]	λ_f (nm)[b]	Φ_f[b]
1	273	5.8×10^4					
	324	3.6×10^4	376, 475		347	475	0.04
	340	3.5×10^4					
1·Cu(II)	275	3.9×10^4					
	337	2.9×10^4	382, 441	3.6×10^4	349	441	0.08
	350	2.7×10^4					
1·Hg(II)	273	4.6×10^4					
	326	3.7×10^4	376, 475, 574[d]		347	475	0.05
	340	3.9×10^4		2.4×10^3			
	554	1.6×10^4			542	574	0.15

[a] Association constants (K_a) from Ref. (*10*).
[b] Fluorescence quantum yields (Φ_f) were calculated according to Ref. (*11*); excitation wavelength (λ_{ex}) and maximum fluorescence wavelength (λ_f).
[c] Fluorescence emissions (λ_{em}, 6 μM) of **1**, **1**·Cu(II) (100 equiv.) and **1**·Hg(II) (100 equiv.) were determined by an excitation at 340 nm.
[d] Fluorescence emissions (λ_{em}, 6 μM) of **1**, **1**·Cu(II) (100 equiv.) and **1**·Hg(II) (100 equiv.) were determined by an excitation at 520 nm.

As noted above, it is conventionally considered that the Py forms two types of excimers, *dynamic* (*6*) and *static* (*7*). Here, with an excitation at 340 nm, we observed an increased emission of the pyrenyl excimer when only one equivalent of Cu(II) ion was added to **1**. In the absence of the metal ion, its fluorescence (pyrenyl excimer emission) is weak due to the photoinduced electron transfer (PET) from the nitrogen atom of the tren part to the excited state of the Py fluorophore. However, the complexation of the nitrogen atoms by Cu(II) ion inhibits PET, but there is a metal ion-induced chelation-enhanced fluorescence (CHEF) effect that induces fluorescence enhancements. Upon further addition of Cu(II) ion, the monomer emission of **1** increases while the associated excimer emission (475 nm) decreases along with a band shift to 441 nm (Figure 2(b)). The diminished excimer emission can be explained by the 'dimeric' formation of the two Py units of **1** in the ground state (Scheme 2). In order to elucidate these unexpected results, we took the excitation spectra of **1**. We then found that the excitation spectra (*13*) of **1**·Cu(II) excited at 376 nm (monomer) differ from that excited at 441 nm (excimer; Figure S6, available online). Therefore, one can conclude that the chemical species for 441 nm are different from that for 376 nm emission. This is an explicit evidence for the formation of pyrenyl *static* excimer of **1** in the event of Cu(II) ion binding (*7*).

We also prepared **2** having only one Py pendent. In fact, **2** shows only a Py monomer emission band excluding the exciplex and the excimer band of Py at 441 nm (Figure S7, available online). Thus, it should be noteworthy that in **1**·Cu(II), the blue-shifted emission band showing at 441 nm is logically assigned to the pyrenyl *static* excimer as seen in Scheme 2.

Upon addition of Hg(II) ion, **1** shows no changes in the Py absorption band (273–340 nm), but it does show new small band at 554 nm, which corresponds to the rhodamine absorption band (Figure 3). The fluorescence intensities of both pyrenyl monomer and excimer increase mainly due to the CHEF executed from Hg^{2+}-bound tren nitrogen to Py arms (*4*, *12*). In addition, the solution of **1** shows a colour change from colourless to pink. The fluorescence emission of the rhodamine was also observed at 574 nm

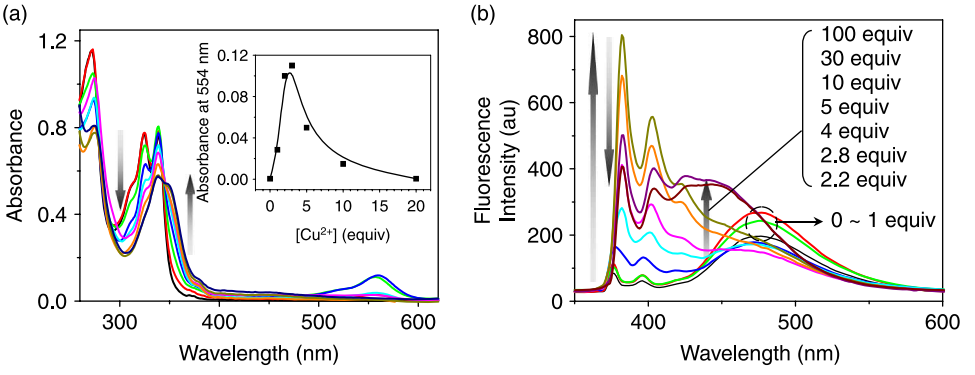

Figure 2. (a) Absorption (20.0 μM) and (b) fluorescence (6.0 μM) spectra of **1** upon addition of various amounts of $Cu(ClO_4)_2$ in CH_3CN, $\lambda_{ex} = 340$ nm. Inset: titration profile of fluorescence intensity at 554 nm *vs.* $[Cu^{2+}]$.

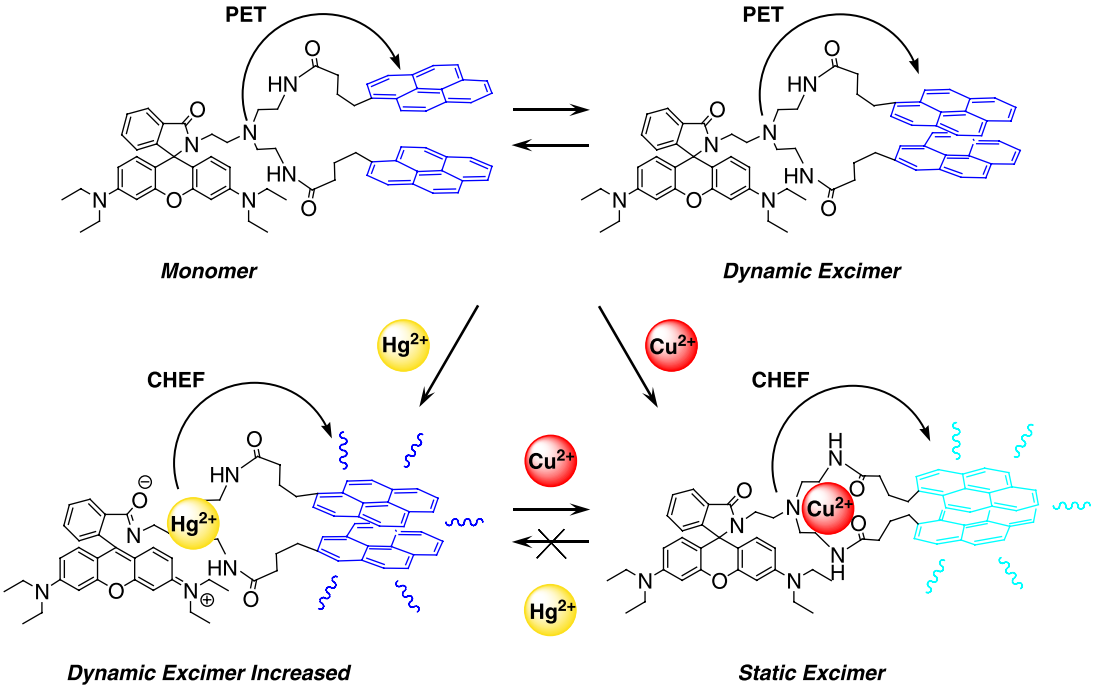

Scheme 2. Schematics of the formation of *dynamic* and *static* excimers depending on the metal ion species ($\lambda_{ex} = 340$ nm).

with an excitation at 520 nm (Figure S8, available online). From this spectral changes, one can assume that the Hg(II) ion is bound predominantly to the rhodamine carboxyl group rather than to the pyrenyl amide part (Scheme 2).

For further application, we prepared a mixed solvent, e.g. H_2O:CH_3CN, but the desired pattern such as ratiometry or characteristic dynamic and static excimer emissions upon metal ion complexation has not been shown. Therefore, we have used a sole solvent, CH_3CN, in this fluorescence study, even though the application aspect seems to be rather deficient.

As we have mentioned above, addition of Hg(II) to **1** also promotes significant changes in the UV/vis and fluorescence spectra in comparison with those observed when Cu(II) was added. However, we found the photochemical binding mechanism of **1** is dependent on the binding of the metal ion species: Cu(II) or Hg(II).

To obtain an insight into a binding mode of the **1** · Hg(II) ion, ^{1}H NMR experiments were carried out (Figure S9, available online). For free **1**, the chemical shift of tren NH is 7.3 ppm, whereas, in the presence of $Hg(ClO_4)_2$, it was broadened and shifted to 9.5 ppm. The aromatic protons in the rhodamine (H_{a-f}) also reveal distinct chemical shift changes. These results support that both the spirolactam carboxyl groups in the rhodamine and tren part are involved in the Hg(II) binding to induce a ring opening of spirolactam in **1**.

The excimer emission changes of **1** based on the metal ion exchange were monitored by titrating Cu(II) ion to a solution of **1** · Hg(II) (Figure S10, available online). When

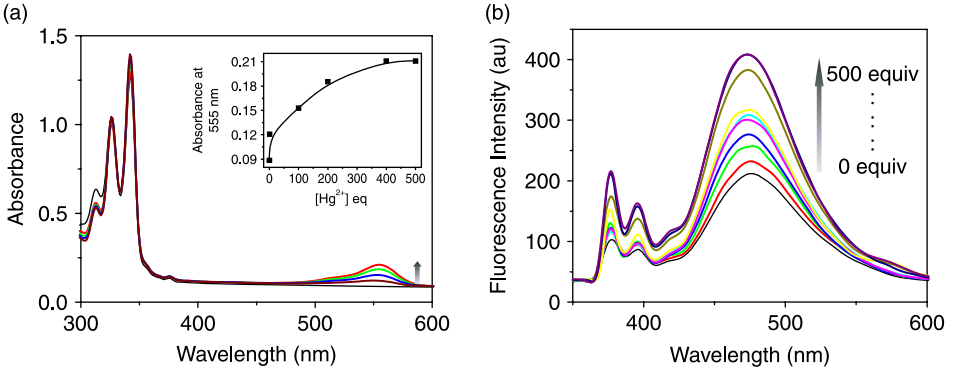

Figure 3. (a) Fluorescence (6.0 μM) and (b) absorption (20.0 μM) spectra of **1** upon addition of various amounts of $Hg(ClO_4)_2$ in CH_3CN, $\lambda_{ex} = 340$ nm. Inset: titration profiles of absorbance *vs.* [Hg^{2+}].

Cu(II) is added, the *dynamic* excimer band (475 nm) shifts to 441 nm and the red-shifted Py absorption appears at 350 nm (Figure S11, available online). The displacement of Hg(II) by Cu(II) gives a brown complex in which the pyrenylamide-*O* binds the Cu(II) to produce a *static* excimer. However, when the Hg(II) is added to the preformed **1** · Cu(II) complex, the emission bands remain unchanged (Figure S12, available online), both of which means that the binding ability of Cu(II) ion to **1** is better than that of Hg(II).

To elucidate the binding mode of Cu(II) ion to **1**, DFT calculations (*14a*) for the **1** · Cu(II) complex were performed using the Gaussian03 program (*14b*). Ground-state geometry optimisation for the global minimum structure of the **1** · Cu(II) complex in a gas phase has been executed using B3LYP hybrid functional with the 3-21G basis set (*14c*). Several different initial conformations were subjected to energy optimisation to search the primary binding sites for Cu(II) ion to **1.** For each energy minimum structure, vibrational analysis was performed to verify the identity of each stationary point as a minimum. For the thermodynamic stability comparison, single point energy calculation was executed at the MPWB1K/3-21G level (*14d*) using B3LYP/3-21G optimised geometry.

In Figure 4(a), the lowest energy structure at the B3LYP/3-21G level for the **1** · Cu(II) complex shows that Cu(II) ion is bound to the two pyrenylamide group oxygens of **1**, with the average distance of 1.74 Å. On the other hand, as shown in Figure 4(b), when Cu(II) ion is encapsulated to the rhodamine carboxyl group oxygen of **1**, the spirolactam ring opening is induced to give a quinonoid rhodamine resulting in a higher energy of 20.5 kcal/mol when compared with the structure in Figure 4(a) at the MPWB1K/3-21G//B3LYP/3-21G level. This computational result that Cu(II) ion thermodynamically prefers to bind to the pyrenylamide oxygens instead of the rhodamine carboxyl oxygen is in excellent agreement with the experimental observation.

Also, the fluorescence behaviour of **1** upon Cu(II) complexation was characterised by performing a time-dependent density functional theory (TDDFT) calculations based on the S_0 state of both structures in Figure 4 (*14e*). On the basis of the TDDFT/B3LYP/3-21G calculation, only for the structure in Figure 4(a), an appreciable excitation probability was found for a HOMO–LUMO interaction between one Py and the other Py (Py–Py*), presumably contributing to the strong fluorescence static excimer band in the **1** · Cu(II) complex (Figure S19, available online).

Conclusions

New synthetic receptor **1** shows a binding selectivity for Hg(II) and Cu(II) ions with respect to both the absorption and emission spectral changes. We herewith explicitly elucidate the binding mechanism of **1** for each metal ion by the absorption and emission spectral changes as well as by the DFT calculation method. From the spectral changes, we found that there is a unique regio-selective binding of **1** for metal ions. In the competition experiment, Hg(II) in the **1** · Hg(II) complex can be readily replaced by Cu(II), and then the static excimer emission of two Pys in **1** is reformed. This significantly means that sensor **1** can therefore be used for Cu(II) sensing, although other metal ions including Hg(II) are present.

Experimental section

Synthesis

Preparation of **1**

Rhodamine **3** (0.40 g, 0.70 mmol) and 1-pyrenebutyric acid (0.50 g, 1.8 mmol) were dissolved in THF (10 ml) and stirred for 5 min under N_2, and then DCC (0.22 g, 1.05 mmol) and DMAP were simultaneously added. The reaction mixture was stirred for 3 h at 50°C and for

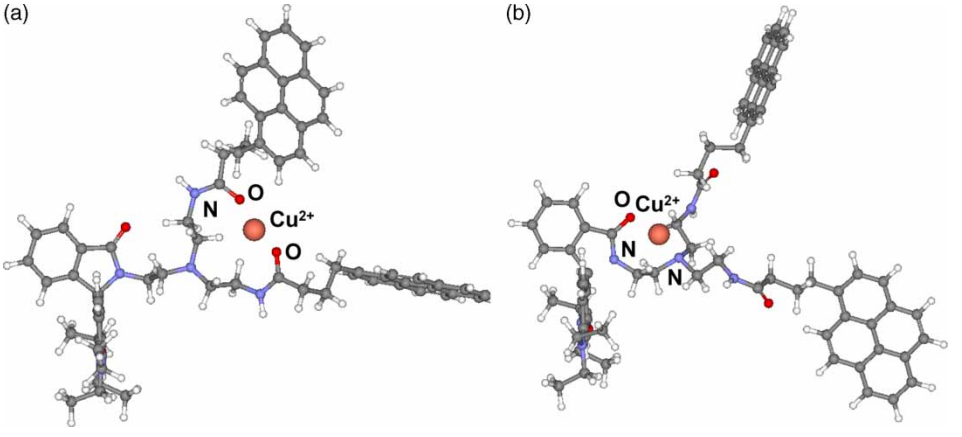

Figure 4. B3LYP/3-21G optimised structures for the **1** · Cu(II) complexes: (a) Cu(II) ion is bound to the two pyrenylamide group oxygens of **1** and (b) Cu(II) ion is bound to the rhodamine carboxyl group oxygen of **1**.

an additional 24 h at room temperature. The precipitate was removed by filtration. After the THF was removed *in vacuo*, CH_2Cl_2 and water were added and the crude product was extracted to the organic layer. Removal of the solvent *in vacuo* gave a brownish crude, which was purified by column chromatography on silica gel (methylene chloride/methanol, 10:1) to provide 0.38 g of **1** in 40% yield as a brownish solid. M.p. 116–120°C. IR (KBr pellet, cm^{-1}): 3293, 1659, 1515; ^1H NMR ($CDCl_3$, 200 MHz): δ 8.24 (d, 2H, $J = 9.20$ Hz), 8.10–7.85 (m, 14H), 7.79 (d, 2H, $J = 7.80$ Hz), 7.56 (m, 3H), 7.38 (t, 1H, $J_1 = 7.20$ Hz, $J_2 = 16.60$ Hz), 7.07 (m, 2H), 6.29 (d, 2H, $J = 0.01$ Hz), 6.20 (d, 2H, $J = 9.40$ Hz), 5.95 (m, 2H), 3.22 (m, 12H), 3.12 (s, 2H), 2.47 (m, 4H), 2.37 (s, 4H), 2.15 (m, 4H), 1.98 (s, 2H), 1.70 (s, 4H), 1.05 (t, 12H, $J_1 = 7.20$ Hz, $J_2 = 7.00$ Hz). ^{13}C NMR ($CDCl_3$, 50 MHz): 173.2, 168.6, 153.5, 152.6, 148.7, 136.3, 131.3, 130.8, 129.7, 128.6, 127.4, 126.4, 125.6, 124.6, 123.4, 108.1, 104.9, 97.4, 66.0, 53.2, 48.8, 44.2, 36.7, 36.1, 33.9, 33.1, 30.9, 27.8, 25.6, 24.9, 12.4 ppm; FAB-MS *m/z* (M^+) calcd 1110.58, found 1111.00.

Preparation of **2**

Similar synthetic methods to **1** were applied. Brownish solid in 36% yield (0.20 g). M.p. 120–126 ?. IR (KBr pellet, cm^{-1}): 3295, 1659, 1513; ^1H NMR ($CDCl_3$, 200 MHz): δ 8.31–7.80 (m, 10H), 7.40 (m, 2H), 7.07 (m, 1H), 6.64 (s, 1H), 6.41–6.12 (m, 6H), 3.39–3.24 (m, 14H), 2.62 (m, 2H), 2.40–2.20 (m, 6H), 1.09 (t, 12H, $J_1 = 6.80$ Hz, $J_2 = 6.99$ Hz). ^{13}C NMR ($CDCl_3$, 50 MHz): 177.8, 176.0, 173.0, 169.1, 153.5, 148.8, 136.2, 132.6, 130.9, 128.6, 127.5, 126.5, 124.8, 123.9, 122.6, 97.6, 65.3, 44.3, 36.2, 33.1, 28.7, 28.7, 27.6, 12.5 ppm; FAB-MS *m/z* (M^+) calcd 798.02, found 798.00.

Preparation of **3**

This compound was prepared according to a slight modification of the literature procedure (*15*). Under nitrogen, a solution of rhodamine B (0.40 g, 0.84 mmol) and tren (0.24 g, 1.68 mmol) in methanol (20 mL) was heated at 80°C. After cooling to room temperature, the solvent was evaporated *in vacuo*. CH_2Cl_2 (100 mL) and water (200 mL) were added, and the organic layer was separated. The CH_2Cl_2 layer was washed twice with water, followed by drying over anhydrous Na_2SO_4. After filtration of sodium sulphate, removal of the solvent *in vacuo* gave 0.40 g of **3** as a colourless oil in 85% yield. IR (KBr pellet, cm^{-1}): 3352, 1683, 1615, 1515; ^1H NMR ($CDCl_3$, 200 MHz): δ 7.90 (m, 1H), 7.46 (m, 2H), 7.10 (m, 1H), 6.43–6.29 (d, 6H, $J_1 = 8.8$ Hz, $J_2 = 5.6$ Hz), 3.18 (t, 2H), 2.56 (t, 4H), 2.38–2.21 (m, 6H), 1.60–1.40 (br s), 1.20–1.13 (t, 12H, $J = 6.90$ Hz). ^{13}C NMR ($CDCl_3$, 50 MHz): 167.6, 153.4, 148.8, 132.2, 131.6, 128.9, 128.1, 123.7, 122.6, 108.1, 105.6, 97.6, 64.9, 56.8, 44.3, 39.5, 38.1, 12.5 ppm; FAB-MS *m/z* (M^+) calcd 570.37, found 571.00.

Preparation of **4**

Similar synthetic methods to **3** were applied. Colourless oil in 83% (0.37 g) yield. IR (KBr pellet, cm^{-1}): 3351, 1682, 1612, 1515; ^1H NMR ($CDCl_3$, 200 MHz): δ 7.90 (m, 1H), 7.43 (m, 2H), 7.07 (m, 1H), 6.44–6.23 (m, 6H), 3.37–3.22 (m, 10H), 2.60 (t, 2H, $J_1 = 5.80$ Hz, $J_2 = 5.40$ Hz), 2.54 (t, 4H, $J_1 = 7.00$ Hz, $J_2 = 6.20$ Hz), 1.40–1.30 (br s), 1.18 (t, 12H, $J = 6.80$ Hz). ^{13}C NMR ($CDCl_3$, 50 MHz): 168.6, 167.6, 153.3, 148.6, 132.3, 130.7, 148.6, 132.3, 130.7, 128.4, 128.0, 123.6, 122.6, 107.9, 105.3, 105.1, 97.6, 64.9, 48.7, 47.3, 44.1, 40.0, 12.4 ppm; FAB-MS *m/z* (M^+) calcd 527.33, found 528.00.

Spectroscopic material and methods

Fluorescence emission and UV/vis spectra were conducted on RF-5301-PC and S-2130 instruments, respectively. Stock solutions (10.0 mM) of the hydrated metal perchlorate salts were prepared in CH_3CN. Stock solutions of **1**–**4** were prepared in CH_3CN. For all measurements, the width of the excitation slit is 1.5 nm and that of the emission is 3.0 nm.

Acknowledgements

This work was supported by the SRC (R11-2005-008-02001-0(2008)) and SRC for Women's Diseases at Sookmyung Women's University.

Notes

1. Anthracene ($\Phi_f = 0.27$ in hexane) (*10a*) and Rhodamine 6G ($\Phi_f = 0.90$ in water) (*10b*) were used as the actinomer for the Φ_f of Pyrene and rhodamine B, respectively.
2. Association constants were calculated by using the computer program ENZFITTER, available from Elsevier-BIOSOFT, 68 Hills Road, Cambridge CB2 1LA, United Kingdom.

References

(1) (a) Czarnik, A.W. *Acc. Chem. Res.* **1994**, *27*, 302–308. (b) Ramamurthy, V.; Schanze, K.S. Photochemistry of Organic Molecules in Isotropic and Anisotropic Media. In *Supermolecular Photochemistry*; Marcel Dekker, 2003; Vol. 9.
(2) de Silva, A.P.; Gunaratne, H.Q.N.; Gunnlaugsson, T.; McCoy, C.P.; Rademacher, J.T.; Rice, T.E. *Chem. Rev.* **1997**, *97*, 1515–1566.
(3) Fabbrizzi, L.; Poggi, A. *Chem. Soc. Rev.* **1995**, *24*, 197–202.
(4) (a) Kim, J.S.; Choi, M.G.; Song, K.C.; No, K.T.; Ahn, S.; Chang, S.-K. *Org. Lett.* **2007**, *9*, 1129–1132. (b) Mei, Y.; Bentley, P.A.; Wang, W. *Tetrahedron Lett.* **2006**, *47*,

2447–2449. (c) Park, S.M.; Kim, M.H.; Choe, J.-I.; No, K.T.; Chang, S.-K. *J. Org. Chem.* **2007**, *72*, 3550–3553.
(5) Prado, E.A.; Yamaki, S.B.; Atvars, T.D.Z.; Zimerman, O.E.; Weiss, R.G. *J. Phys. Chem. B* **2000**, *104*, 5905–5914.
(6) Kim, S.K.; Lee, S.H.; Lee, J.Y.; Lee, J.Y.; Bartsch, R.A.; Kim, J.S. *J. Am. Chem. Soc.* **2004**, *126*, 1649–1650.
(7) (a) Kim, S.K.; Bok, J.H.; Bartsch, R.A.; Lee, J.Y.; Kim, J.S. *Org. Lett.* **2005**, *7*, 4839–4842. (b) Jun, E.J.; Won, H.N.; Kim, J.S.; Lee, K.-H.; Yoon, J. *Tetrahedron Lett*. **2006**, *47*, 4577–4580.
(8) (a) Xiang, Y.; Tong, A. *Org. Lett.* **2006**, *8*, 1549–1552. (b) Albers, A.E.; Okreglak, V.S.; Chang, C.J. *J. Am. Chem. Soc.* **2006**, *128*, 9640–9641.
(9) Wu, D.; Huang, W.; Duan, C.; Lin, Z.; Meng, Q. *Inorg. Chem.* **2007**, *46*, 1538–1540.
(10) (a) Briks, J.B. *Photophysics of Aromatic Molecules*; Wiley-Inter-Science: London, 1970. (b) Maged, D.; Wong, R.; Seybold, P.G. *Photochem. Photobiol.* **2002**, *75*, 327–334.
(11) (a) Berreau, L.M.; Halfen, J.A.; Young, V.G., Jr.; Tolman, W.B. *Inorg. Chem.* **1998**, *37*, 1091–1098. (b) Royzen, M.; Dai, Z.; Canary, J.W. *J. Am. Chem. Soc.* **2005**, *127*, 1612–1613.
(12) (a) Kaur, S.; Kumar, S. *Chem. Commun.* **2002**, 2840–2841. (b) Qi, X.; Jun, E.J.; Xu, L.; Kim, S.-J.; Joong Hong, J.S.; Yoon, Y.J.; Yoon, J. *J. Org. Chem.* **2006**, *71*, 2881–2884. (c) Yoon, S.; Albers, A.E.; Wong, A.P.; Chang, C.J. *J. Am. Chem. Soc*. **2005**, *127*, 16030–16031.
(13) (a) Winnik, F.M. *Chem. Rev.* **1993**, *93*, 587–614. (b) Zimerman, O.E.; Weiss, R.G. *J. Phys. Chem. A* **1998**, *102*, 5364–5374.
(14) (a) Stratmann, R.E.; Scuseria, G.E.; Frish, M.J. *J. Chem. Phys.* **1998**, *109*, 8218–8224. (b) Gaussian 03, revision C.02: Frisch, M.J.; Trucks, G.W.; Schlegel, H.B.; Scuseria, G.E.; Robb, M.A.; Cheeseman, J.R.; Montgomery, J.A., Jr.; Vreven, T.; Kudin, K.; Burant, J.C.; et al. Gaussian, Inc.: Wallingford CT, 2004. (c) Becke, A.D. *J. Chem. Phys.* **1993**, *98*, 5648–5652. (d) Zhao, Y.; Truhlar, D.G. *J. Phys. Chem. A* **2004**, *108*, 6908–6918. (e) Gross, E.K.U.; Kohn, W. *Adv. Quantum Chem.* **1990**, *21*, 255–291.
(15) Yang, J.-S.; Lin, C.-S.; Hwang, C.-Y. *Org. Lett.* **2001**, *3*, 889–892.